Earthquake Engineering, Tenth World Conference © 1992 Balkema, Rotterdam. ISBN 90 5410 060 5

Seismic reliability analyses of large scale lifeline networks taking into account the failure probability of the components

T.Sato & K.Toki
Disaster Prevention Research Institute, Kyoto University, Japan

ABSTRACT : To assess the seismic reliability of large scale lifeline networks and taking into account failure probability of the components, we developed an algorithm which has only polynomial complexity to enumerate paths in the network. Using this algorithm we have developed a new approximate calculation scheme, call the point matching method. The uncertainty of the attenuation law, shear wave velocity of ground and component's failure level are considered to calculate the seismic reliability of the network. A check of applicability of our new method is made by hypothetical seismic reliability analysis of a gas supply network composed of 1765 nodes and 1764 links.

1 INTRODUCTION

Because enumeration of lifeline network states in a seismic environment usually has exponential complexity, seismic reliability analyses of large scale networks have not been feasible as the number of components increases. To overcome this deficiency we proposed an efficient procedure for assessing the seismic reliability of lifeline networks (T.Sato 1984). For a fixed earthquake on an active fault zone, we proved that the network took at most $2n^2 - 2n + 2$ states, n being the number of components. In the algorithm, we used the concept of the critical distance to the earthquake fault (Moghtaderizadeh et al,1981). A network is assumed to consist of links and nodes, and a node and link to fail if the seismic response exceeds a particular level at any point in each component. The intensity of the seismic response, Y, at a particular point in the network components is given through an attenuation law in terms of the earthquake magnitude, M, the shortest distance to the rupture zone,r, and the parameters $C_k(k = 1, 2, \cdots)$ which express the source mechanisms and the effect of local geological parameters around the point. If the network component can sustain the magnitude of response expressed by Y^*, the shortest safe distance (the critical distance) between the component and the fault rupture is inversely solved from the attenuation law

$$r^* = f(M, C_k, Y^*) \qquad (1)$$

The sphere of the radius with this distance centered at the element point defines the transition boundary for the component because it divides three dimensional spare into the component of working and non-working states. The shape of the transition boundary for a node is a sphere. For a link it is a combination of a row of spheres and idealized by a circular cone with spheres at both end provided that there is linearity of the failure distances along the link. An example critical distance r^* obtained from an attenuation curve of strain (full line) and an allowable strain of buried pipe at a certain point ε^* is shown in Fig.1. Because the uncertainties of attenuation law and allowable strain of the component are not considered, the failure probability of the component changes from 0.0 to 1.0 if the shortest distance to an earthquake fault r become less than r^* as shown in Fig.2.

The purpose of this paper is to relax this binary condition of component's failure probability. The seismic reliability of a network may decrease if we take into account uncertainties of several factors. Especially the effect of uncertainty of attenuation law must be examined carefully.

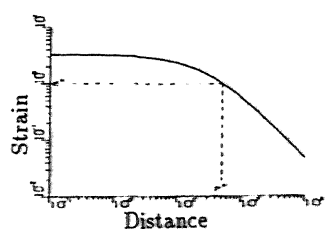

Fig.1 Relation between the seismic pipe strain and critical distance from an earthquake fault

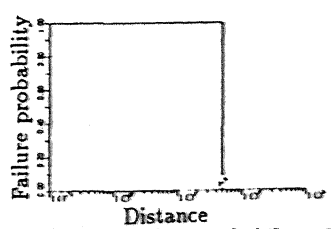

Fig.2 Relation betweenfailure probability of a component and critical distance from an earthquake fault (Not considering uncertainty)

2 DEFINITION OF FAILURE PROBABILITY OF COMPONENT

Network components are assumed to fail when the seismic strain in the pipe exceeds a threshold level or the ground is liquefied. The Japanese specification for the earthquake resistant design of gas pipes (JAPAN GAS Associate 1982) defines the formula with which to calculate pipe strain as

$$\varepsilon = \beta \cdot \delta, \quad \delta = (1-\alpha) \cdot U \tag{2}$$

in which β is the coefficient for transferring relative displacement between the pipe and ground into the pipe strain, α the transmission coefficient, U the ground displacement given by

$$U = \frac{2}{\pi^2} \cdot T \cdot S_V \cdot K \cdot cos(\frac{\pi z}{2H}) \tag{3}$$

in which T is the natural period of the ground, S_V the response velocity value per unit seismic coefficient, K the design seismic coefficient and z the depth of the pipe. By substituting Eq.(3) into Eq.(2) the strain induced in a pipe is expressed as follows:

$$\varepsilon = \beta \cdot (1-\alpha)\frac{2}{\pi^2} \cdot T \cdot S_V \cdot K \cdot cos(\frac{\pi z}{2H}) \tag{4}$$

Because the values of T, S_V and K scatter around their mean values of $\bar{T}, \bar{S_V}$, and $\bar{K}$, Eq.(4) can be rewritten

$$\varepsilon = \beta \cdot (1-\alpha)\frac{2}{\pi^2} \cdot \bar{T} \cdot \bar{S_V} \cdot \bar{K} \cdot cos(\frac{\pi z}{2H}) \cdot \frac{T}{\bar{T}} \cdot \frac{S_V}{\bar{S_V}} \cdot \frac{K}{\bar{K}} \tag{5}$$

Taking logarithm of Eq.(5) the expression of pipe strain is divided into two parts.

$$log\varepsilon = log\{\beta \cdot (1-\alpha)\frac{2}{\pi^2} \cdot \bar{T} \cdot \bar{S_V} \cdot \bar{K} \cdot cos(\frac{\pi z}{2H})\} + log\frac{T}{\bar{T}} + log\frac{S_V}{\bar{S_V}} + log\frac{K}{\bar{K}} \tag{6}$$

The first term of right-hand side Eq.(6) is derived from mean values of parameters. The remaining second, third and forth terms are assumed to be random variables with normal probability distributions $N(\mu_T, \sigma_T^2)$, $N(\mu_{S_V}, \sigma_{S_V}^2)$and $N(\mu_K, \sigma_K^2)$, respectively. If we define ε_0 as follows:

$$\varepsilon_0 = \beta \cdot (1-\alpha^*)\frac{2}{\pi^2} \cdot \bar{T} \cdot \bar{S_V} \cdot \bar{K} \cdot cos(\frac{\pi z}{2H}) \tag{7}$$

$log\varepsilon$ has a normal probability distribution with a mean value of $\mu_\varepsilon = log\varepsilon_0$ and a variance of $\sigma_\varepsilon^2 = \sigma_T^2 + \sigma_{S_V}^2 + \sigma_K^2$. To calculate ε_0 the value of K must be expressed by an attenuation law in terms of the earthquake magnitude, m,and the shortest distance to the rupture zone, r. Because attenuation laws proposed so far are functions of the magnitude and epicentral distance, we have used the following relation for K(K.Kawashima et al 1986)

$$K \cdot g = 227 \cdot 10^{0.308m}(r+30)^{-1.201} \tag{8}$$

in which g is the acceleration of gravity.

The failure probability of a component for an earthquake with magnitude m at critical distance $\bar{r}_1$ is calculated as shown in Fig.3. If the allowable strain level ε^* is a definite value the component loses its function on the condition of $\varepsilon \geq \varepsilon^*$. The failure probability $p_f(m, \bar{r}_1)$ therefore, can be calculated by the area of shaded part in Fig.3 or by the following formula,

$$p_f(m, \bar{r}_1) = P(\varepsilon \geq \varepsilon^*) \tag{9}$$

An example relation between failure probability of a component and the critical distance from an earthquake fault is given in Fig.4. The distance r^* at where the failure probability being 0.5 is obtained from the condition of $\varepsilon_0 = \varepsilon^*$.

If the allowable strain ε^* is a random variable obeying a logarithmic normal distribution with the mean value of $\mu_{\varepsilon^*} = log\bar{\varepsilon}^*$ and the variance of $\sigma_{\varepsilon^*}^2$ then failure probability of the component $p_f(m, \bar{r})$ is given by

$$p_f(m, \bar{r}) = 1.0 - \Phi(\frac{\mu_{\varepsilon^*} - \mu\varepsilon}{\sqrt{\sigma_{\varepsilon^*}^2 + \sigma_\varepsilon^2}}) \tag{10}$$

in which is $\Phi(x)$ the standard normal distribution function.

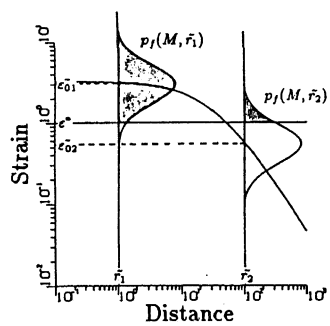

Fig.3 Calculation of failure probability of a component at several critical distances from an earthquake fault

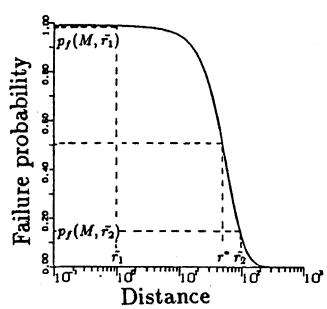

Fig.4 Relation between failure probability of a component and critical distance from an earthquake fault (Taking into account uncertainty)

3 SEISMIC ENVIRONMENT

The gross parameters of the seismic source, which are required to reliability analysis of lifeline network, are the fault length and width, the seismic moment and the magnitude of the earthquake. The seismic moment, M_o is the fundamental parameter used to measure the magnitude of an earthquake caused by a fault slip, but the surface magnitude, m_s, is used in engineering. We have the relation between m_s and M_o given by R.J.Geller(1976).The fault area, S, also is related to M_o ;

$$S = 1.88 \cdot 10^{-15} M_o^{2/3} \tag{11}$$

The network component will fail with probability, $p_f(m, \tilde{r})$,if the transition boundary with the critical distance $\tilde{r}$ intersects the earthquake rupture area.To take into account the probabilistic nature of an earthquake occurring, we have defined an active fault zone. The collocation of earthquake rupture on this active fault zone is determined from a probabilistic concept. We assume rectangular areas (the length of fault to be twice of the width)for the active fault zone and for a rupture caused by an earthquake as shown in Fig.5. The collocation of both rectangles is arranged with the axes of symmetry parallel. We define the transition area with failure probability of $p_f(m, \tilde{r})$ as the intersection between the transition boundary of a component of the network and the active fault zone as shown in Fig.5. For a node it is a circle; for a link it is the cross section between the active fault plane and a circular cone with a sphere at both end. To formulate network reliability, we must assume that this transition area with failure probability p_f may intersect an earthquake rupture with magnitude m; therefore, it is convenient to look at the positions of rupture from the center of the earthquake. We defined a coordinate transformation (T.Sato 1984) by which the position of earthquake rupture can be represented by the center of the rupture.

An example of the collocation of this newly defined transition area for a simple network composed of twelve nodes and eleven links is shown in Fig.6. We assume that only transition boundaries of nodes D and E compose transition areas. The relation between the failure probability and critical distance was a continuous function as shown in Fig.4. For purpose of numerical simplicity we discretize this relation as shown in Fig.6. There are four transition areas for each node with different failure probability and these areas divide the active fault zone into 12 regions (define as influence regions) that are mutually exclusive and collectively exhaustive regions. The network condition changes from one region to the other. For example the region 8 expresses the network condition that nodes of D and E fail simultaneously with probabilities of 0.5 and 0.25, respectively.

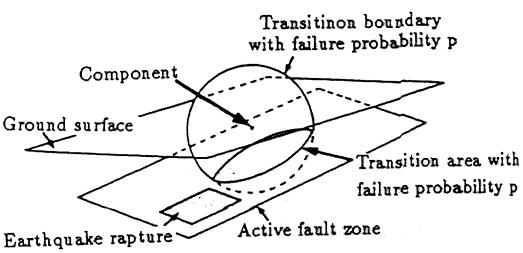

Fig.5 Collocation of transition boundary, an earthquake rapture in the active fault zone and transition area of a component

4 NETWORK RELIABILITY COMPUTATION

In order to illustrate the reliability computation a multi-terminal reliability measure is used that is defined as the probability that the given source nodes can be connected to all specified terminal nodes in the network. Let $I_i(x, y/m)$ be an reliability index of influence region i defined by the probability to satisfy the function of a network after a magnitude m earthquake with a rupture centered at (x, y). How to calculate the reliability index of region $8(I_8)$ in Fig.6 is explained in Table 1. The connectivity from nodes A and B to nodes K and L is chosen as the reliability measure. These are four cases based on components failure condition. $I_8(x, y/m)$ becomes 0.75 by adding all probabilities of network functioning.

For simplicity we consider only one active fault zone in the following analysis. The transition areas divide the active fault zone into some M influence regions $A_i (i = 1, 2, \cdots, M)$. Each A_i, region corresponds to some state of the network and $I(x, y/m)$

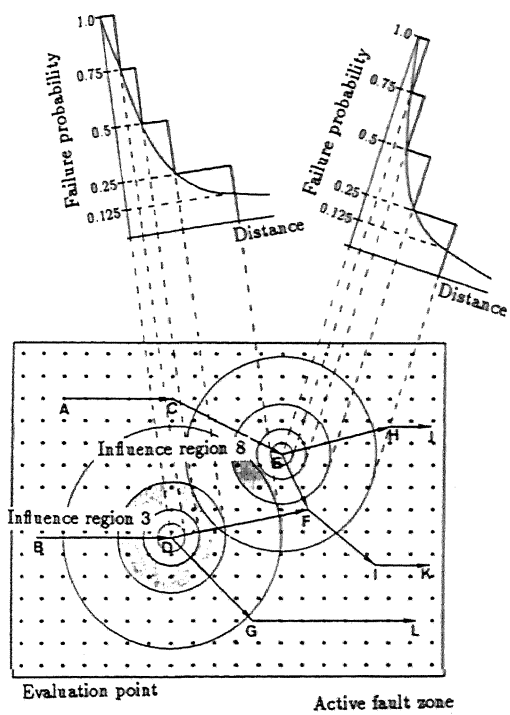

Fig.6 Example of the collocation of transition area with different failure probability for simple network (Only the transition areas of nodes D and E are con-

is constant within A_i so that the reliability of the network, G, conditioned on magnitude m is

$$R(G/m) = \sum_{i=1}^{M}\{I_i(A_i/m) \cdot A_i\} / \sum_{i=1}^{M} A_i \qquad (12)$$

in which we assume uniform distribution of earthquake occurrence on the active fault zone.

4.1 Point matching method

The most time consuming part of the developed program is the calculation of area of influence region A_i. After detail check of program statements we found that the order of enumeration for a network with n elements was $O(n^6)$ due to the existence of nested DO ROOPS to calculate A_i although our algorithm guarantees the order of $O(n^2)$. To overcome this deficiency we have developed an algorithm named "point matching method". The idea of the method is simple. Evaluation points are uniformly distributed on the active fault zone and the area of region A is assumed to be proportional to the number of evaluation points included in the region A_i. The value of reliability index defined by $I(x, y/m)$ is assumed to each evaluation point. If the number of evaluation points in the region A_i is N_i then Eq(12) is rewritten as follows :

$$R(G/m) = \sum_{i=1}^{M}\{I_i(N_i/m) \cdot N_i\} / \sum_{i=1}^{M} N_i \qquad (13)$$

The reliability for the network shown in Fig.6 is calculated in Table 2 using the above mentioned procedure. The number of evaluation points is 300 and the included evaluation points in each influence region is also given in Table 2.

Table 1 Calculation of reliability index

	Node D	Node E	Reliabilty measure	Probability
1	F	F	NS	
2	F	F	NS	
3	NF	F	S	$(1-0.25) \times 0.5 = 0.375$
4	NF	NF	S	$(1-0.25) \times (1-0.5) = 0.375$
				Reliability index $I_s = 0.750$

F: S: Satisfy

Nf: Non failure NS: Not satisfy

Table 2 Calculation of reliability for the connectivity from nodes A and B to nodes K and L

Region No.	Reliablity index I_i	Number of evaluation points N_i	$N_i \cdot I_i$
1	1.0	177	177
2	0.75	44	33
3	0.5	12	6
4	0.25	6	1.5
5	0.0	1	0
6	0.5	2	1
7	0.75	11	8.25
8	0.75	2	1.5
9	1.0	31	31
10	1.0	8	8
11	1.0	4	4
12	1.0	2	2
Total		300	273.25
		Reliability	$R = (\sum_{i=1}^{12} I_i \cdot N_i) / \sum_{i=1}^{12} N_i = 0.9108$

4.2 Application of minimal cutset

In Table 1 we counted out all possible case for calculating reliability index. But this is not feasible as the number of collectively exhaustive regions increases. For an illustrative purpose a network shown in Fig.7 is considered. The reliability measure is connectivity from nodes S_1, S_2, and S_3 to nodes D_2 and D_3. The transition areas of nodes A, B, C and D are intersected with active fault zone and only single failure probability for each transition area is assigned as given in Table 3. If we calculate the reliability index of shaded influence region by taking into account all possible cases we have to count out 16 (2^4) cases because this region is included inside of four transition areas composed of nodes A, B, C and D. The computation time to calculate the reliability index expands exponentially as the number of related transition areas of an influence region increases. To avoid this difficulty we use minimal cutset which is the subset of network components. If only one component in this subset survives the connectivity of the network is satisfied. In the example given in Table 4 the minimal cutset is the combination of nodes C and D because both nodes must survive to satisfy the reliability measure. The reliability index of this influence region, therefore, can be calculated by counting out all cases satisfying reliability measure for nodes A and B and multiplying survival probability of nodes C and D as shown in Table 5.

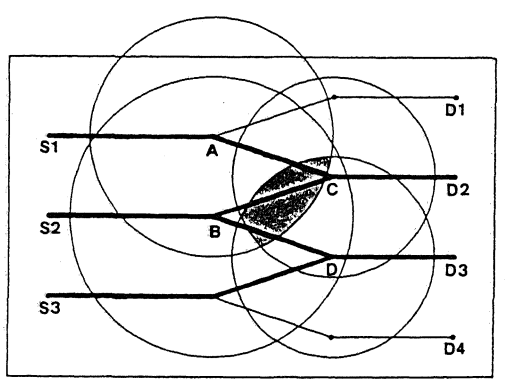

Fig.7 A network to apply the minimal cutset

Table.3 Failure probability and survival probability

Node	P_f	P_l
Node A	0.3	0.7
Node B	0.4	0.6
Node C	0.9	0.1
Node D	0.8	0.2

Table.4 Calculating reliability index without using minimal cutset

	Node A	Node B	Node C	Node D	Reliability measure	Probability
1	o	o	o	o	o	0.7×0.6×0.1×0.2=0.0084
2	o	o	o	×	×	
3	o	o	×	o	×	
4	o	o	×	×	×	
5	o	×	o	o	o	0.7×0.4×0.1×0.2=0.0056
6	o	×	o	×	×	
7	o	×	×	o	×	
8	o	×	×	×	×	
9	×	o	o	o	o	0.3×0.6×0.1×0.2=0.0036
10	×	o	o	×	×	
11	×	o	×	o	×	
12	×	o	×	×	×	
13	×	×	o	o	×	
14	×	×	o	×	×	
15	×	×	×	o	×	
16	×	×	×	×	×	
						Reliability index 0.0176

Table.5 Calculation of reliability index using minimal cutset

	Node A	Node B	Reliability measure	Probability
1	o	o	o	0.7×0.6=0.42
2	o	×	o	0.7×0.4=0.28
3	×	o	o	0.3×0.6=0.18
4	×	×	×	
				0.88
			Reliability index	0.1×0.2×0.88=0.0176

5 A MODEL OF GAS NETWORK AND AN ACTIVE FAULT ZONE

We considered a gas supply network (Fig.8) composed of 1765 nodes and 1764 links. The network shown in Fig.8 is an idealization of the southern portion of the middle pressure A line (gas pressure; $10 > p > 3kg/cm^2$)and B line ($3 > p > 1kg/cm^2$). Six source nodes expressed by astrisks are connected to the high pressure line through regulator stations, and 640 terminal nodes are connected to source nodes of the low pressure line ($p < 1kg/cm^2$) through district regulators. Based on the gas demand 116 terminal nodes are chosen as the demand nodes. To evaluate the reliability of this network we have chosen a simple connectivity measure, the probability that gas can reach all the demand nodes. An active fault zone is considered (Fig.9). This zone includes the fault area of the 1923 Kwanto Earthquake.The shear wave velocity and thickness of the ground at each node are determined by using the geological data base constructed from the results of standard penetration tests conducted at 1618 points in the area concerned. The depth of the buried pipe elements is assumed to be 1.2m.

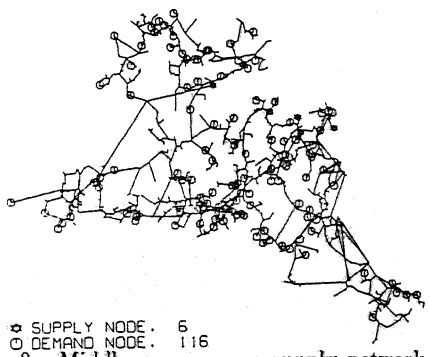

Fig.8 Middle pressure gas supply network model in Shounan area
(6 supply nodes and 116 demand nodes)

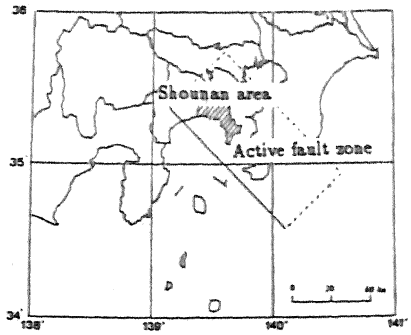

Fig.9 An active fault zone

6 COMPARISON OF CPU TIME FOR EXECUTING THE PROGRAM

The main system of the data processing center of Kyoto University consists of a largescale general-purpose computer, FACOM M-780/30 and two super computers, VP-400E and VP-200. We use M-780/30 and VP-400E system for comparing CPU time to analyze seismic reliability of a sample network. A fortran program developed by using M-780/30 can be executed by a vectorized computer (VP-400E) without any modification. Decrease of execution time is based on the rate of vectorization of each program unit. To decrease efficiently execution time of the program unit there is a software with an interactive capability, to show the execution time of each program unit on VP-400E and on M-780/30; the number of execution times of each program unit; a possibility for vectorization and procedures to increase computation speed of each program unit.A comparison of needed CPU time between a vectorized computer (VP-400E) and a general purpose computer (M-780/30) for analyzing seismic reliability of a gas supply network with the 3529 elements gives a result that the vectorized program attains 5.5 times computation speed at the magnitude of 7.0. As the earthquake magnitude becomes large the efficiency of vectorized program increases because the vectorized length(the number of data processed by vectorizer)becomes long.

To check the accuracy of the point matching method the seismic reliability of above mentioned gas supply network is calculated for earthquake magnitude of 6.6, 6.8 and 7.0. The number of evaluation points is 5000. The results also show in good agreement between the seismic reliability calculated by the exact method and that by the point matching method. Although the program of this method is executed on M-780/30, the CPU time is attained almost 6 times

lesser than that for exact solution obtained by using super computer (VP-400E).

7 APPLICATION

A work station, NEWS-1860, with 5.3 MIPS processing speed is mainly used for calculating seismic reliability of the gas network shown in Fig.8. In the network there are 640 terminal nodes. We classified tease terminal nodes into five levels based on their gas demands. The case of 116 demand nodes is the fourth level. The standard deviations of random valuables appeared in Eqs.(6) and (10) are determined by using the observed and experimental data as follows:

$$\sigma_T = 0.151, \quad \sigma_{S_V} = 0.105,$$

$$\sigma_K = 0.244, \quad \sigma_{\epsilon^*} = 0.04$$

The relation between the failure probability of a component and critical distance is discretized every 1% level. The calculated seismic reliability against a random earthquake for the fourth level of demand is shown in Fig.10. Three cases are presented in the figure. First is the case of without any uncertainties, so that only the binary failure probability for each component is assumed. Second is that of taking into account only the uncertainty of attenuation law, and third includes all uncertainties. Because the uncertainty of attenuation law is largest the seismic reliability of network decreases drastically when the uncertainty of attenuation lawtakes into account. The

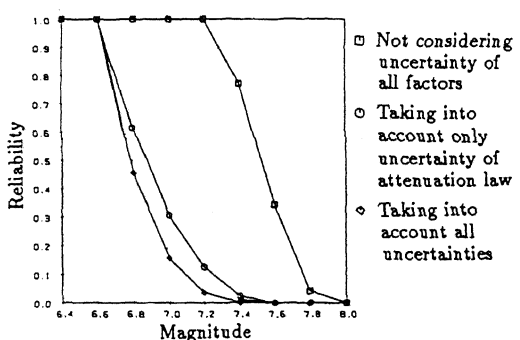

Fig.10 Relation between seismic reliability and earthquake magnitude

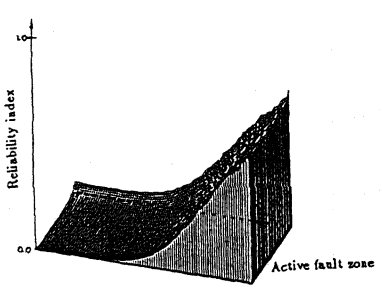

Fig.11 Distribution of seismic reliability index on the active fault zone

distribution of reliability index on the active fault zone is calculated for each earthquake magnitude as shown in Fig.11. This is the result for earthquake magnitude 7.0. The probability density function of seismic reliability of the network is obtained from Fig.11 as shown in Fig.12 based on Eq.13. By integrating the probability density function we can draw the cumulative distribution function of seismic reliability of network as shown in Fig.13. From this figure we can estimate the probability guaranteeing a certain level of seismic reliability of network.

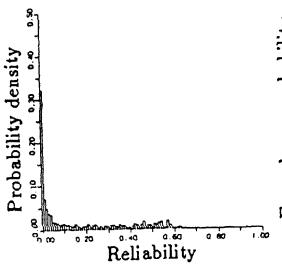

Fig.12 Probability density of seismic reliability

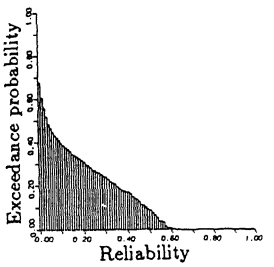

Fig.13 Cumulative distribution of seismic reliability

8 CONCLUSION

Uncertainties of several factors for assessing seismic reliability of large scale lifeline system have been implemented in the algorithm with which to analyze the seismic reliability. It uses a new approximate calculation scheme called point matching method and minimal cutset theory. Calculation of the seismic reliability of an example network shows that newly developed program package can be used with large networks. The result reveals that the effect of uncertainty of attenuation law is the largest on the seismic reliability analyses of networks.

REFERENCES

Sato,T., "Seismic reliability analysis of lifeline networks taking into account fault extent and local ground conditions", Natural Disaster Science, Vol.6,No.2,51-72,(1984).

Moghtaderizadeh,M.,Wood,R.K.,Der Kiureghian,A., Barlow,R.E.and Sato,T., " Seismic reliability of flow and communication networks ", Lifeline Earthquake Engineering, The Current State of Knowledge, ASCE,81-96(1981).

Japan Gas Association,"Specification for earthquake resistant design of gas pipelines", March(1982)(in Japanese).

Kawashima,K.,Aizawa,K.andTakashina,K.,"Attenuation of peak ground acceleration,velocity and displacement based on multiple regression analysis of Japanese strong motion records", Earthquake Engineering and Structural Dynamics,Vol.14,pp.199-215 (1986).

Geller,R.J.,"Scaling relation for earthquake source parameters and magnitude", Bull. Seism.Soc. America, Vol.66, No.5, pp.1501-1523 (1976).